Anisotropic compact stars in Karmarkar spacetime

Ksh. Newton Singh[1;1)]   Neeraj Pant[2;2)]   M. Govender[3;3)]

[1] Department of Physics, National Defence Academy, Khadakwasla, Pune-411023, India
[2] Department of Mathematics, National Defence Academy, Khadakwasla, Pune, 411023, India
[3] Department of Mathematics, Faculty of Applied Sciences, Durban University of Technology, Durban, South Africa

Abstract: We present a new class of solutions to the Einstein field equations for an anisotropic matter distribution in which the interior space-time obeys the Karmarkar condition. The necessary and sufficient condition required for a spherically symmetric space-time to be of Class One reduces the gravitational behavior of the model to a single metric function. By assuming a physically viable form for the g_{rr} metric potential we obtain an exact solution of the Einstein field equations which is free from any singularities and satisfies all the physical criteria. We use this solution to predict the masses and radii of well-known compact objects such as Cen X-3, PSR J0348+0432, PSR B0943+10 and XTE J1739-285.

1   Introduction

The century-old search for exact solutions of the Einstein field equations began with Karl Schwarzschild obtaining a vacuum solution describing the exterior of a spherically symmetric matter distribution [1]. A natural line of pursuit would be to find an interior solution which matched smoothly to the Schwarzschild exterior solution. This internal solution was obtained by Schwarzschild, in which he assumed that the internal matter content of a spherical mass distribution was characterized by uniform density [2]. Observations of stars and the understanding of particle physics within dense cores necessitated the search for more realistic solutions of the field equations. The inclusion of pressure anisotropy, charge, bulk viscosity, an equation of state, multilayered fluids and the departure from spherical symmetry has led to the discovery of hundreds of exact solutions describing relativistic stars in the static limit [3–7]. With the discovery of the Vaidya solution, it became necessary to model the gravitational collapse of radiating stars [8]. Since the star is dissipating energy in the form of a radial heat flux, the pressure at the boundary of the star is proportional to the outgoing heat flux as opposed to vanishing surface pressure in the non-dissipative case [9]. Nevertheless, static solutions also play a pivotal role in dissipative gravitational collapse of stars as they can represent an initial static configuration or a final static configuration [10–12].

Relaxing the condition of a perfect fluid and allowing for pressure anisotropy and charge within the interior of the stellar distribution gives rise to observable and measurable properties of the star. Pressure anisotropy leads to arbitrarily large surface red-shifts [13–15] while the inclusion of charge results in the modification of the Buchdahl limit ([16]). The linear equation of state $p = \alpha\rho$ has been generalized from observations in theoretical particle physics. There has been a wide spectrum of exact solutions of the field equations incorporating the so-called MIT bag model, in which the equation of state is of the form $p = \alpha\rho - B$ with B being the bag constant [17–19]. These solutions successfully predicted the observed masses and radii of compact objects with densities of the order of 10^{14} g·cm^{-3}. With an ever growing interest in dark energy and its successful use in cosmological models, astrophysicists have now extended the range of α in $p = \alpha\rho$ to include $-1 < \alpha < -1/3$. This regime incorporates the so-called dark stars [20, 22]. Other exotic forms of matter which have appeared in the literature include the Chaplygin gas, Bose-Einstein condensates and the Hagedorn fluid [23–27].

The notion of the four fundamental interactions being a manifestation of a single force has always attracted the interest of researchers in both fundamental particle physics and relativity. Higher dimensional theories of gravity have produced rich results so far as cosmic cen-

sorship is concerned [28–30]. Recently, there has been a surge in exact models of stars in Einstein-Gauss-Bonnet gravity and braneworld gravity as well as Lovelock gravity [31–34]. The connection between five-dimensional Kaluza-Klein geometries and electromagnetism has been widely studied. Embedding of four-dimensional space-times into higher dimensions is an invaluable tool in generating both cosmological and astrophysical models. In this paper we utilize the Karmarkar [35] condition, which is a necessary and sufficient condition for a spherically symmetric line element to be of class one to generate exact solutions of the Einstein field equations. In particular, our model incorporates anisotropic pressure and is free from any singularities. Our results support recent observations made by Refs. [36–38] for models in embedding Class One.

2   Interior space-time

The interior of the super-dense star is assumed to be described by the line element

$$ds^2 = e^{\nu(r)}dt^2 - e^{\lambda(r)}dr^2 - r^2(d\theta^2 + \sin^2\theta d\phi^2). \quad (1)$$

The energy-momentum tensor for the stellar anisotropic fluid is

$$T_{ab} = \mathrm{diag}\,(\rho, -p_r, -p_t, -p_t), \quad (2)$$

where ρ, p_r and p_t are the energy density, radial pressure and tangential pressure, respectively.

The Einstein field equations for the line element (1) are

$$8\pi\rho = \frac{1 - e^{-\lambda}}{r^2} + \frac{\lambda' e^{-\lambda}}{r} \quad (3)$$

$$8\pi p_r = \frac{\nu' e^{-\lambda}}{r} - \frac{1 - e^{-\lambda}}{r^2} \quad (4)$$

$$8\pi p_t = \frac{e^{-\lambda}}{4}\left(2\nu'' + \nu'^2 - \nu'\lambda' + \frac{2\nu'}{r} - \frac{2\lambda'}{r}\right) \quad (5)$$

where primes represent differentiation with respect to the radial coordinate r. In generating the above field equations we have utilized geometrized units where G and c are taken to be unity. Using the Eqs. (4) and (5) we obtain the anisotropy parameter

$$\Delta = 8\pi(p_t - p_r)$$
$$= e^{-\lambda}\left[\frac{\nu''}{2} - \frac{\lambda'\nu'}{4} + \frac{\nu'^2}{4} - \frac{\nu' + \lambda'}{2r} + \frac{e^\lambda - 1}{r^2}\right]. \quad (6)$$

If the metric given in (1) satisfies the Karmarkar condition [35] , it can represent an embedding Class One spacetime i.e.

$$R_{1414} = \frac{R_{1212}R_{3434} + R_{1224}R_{1334}}{R_{2323}} \quad (7)$$

with $R_{2323} \neq 0$ [39]. This condition leads to a differential equation given by

$$\frac{2\nu''}{\nu'} + \nu' = \frac{\lambda' e^\lambda}{e^\lambda - 1}. \quad (8)$$

On integration we get the relationship between ν and λ as

$$e^\nu = \left(A + B\int\sqrt{e^\lambda - 1}\;dr\right)^2 \quad (9)$$

where A and B are constants of integration.

By using (9) we can rewrite (6) as

$$\Delta = \frac{\nu'}{4e^\lambda}\left[\frac{2}{r} - \frac{\lambda'}{e^\lambda - 1}\right]\left[\frac{\nu' e^\nu}{2rB^2} - 1\right]. \quad (10)$$

3   Anisotropic stellar solution

To solve the above equation (9), we have assumed an entirely new type of g_{rr} metric potential given by

$$e^\lambda = \frac{4(1 + ar^2)^2}{(2 - ar^2)^2}. \quad (11)$$

On integrating (9), we get

$$e^\nu = \left[A + \frac{B}{\sqrt{a}}\left\{\sqrt{12 + 3ar^2}\right.\right.$$
$$\left.\left. -3\sqrt{2}\;\tanh^{-1}\left(\frac{\sqrt{4 + ar^2}}{\sqrt{6}}\right)\right\}\right]^2. \quad (12)$$

Now using (12) and (11) in (3), (4), (10) and (5), we get

$$8\pi\rho = \frac{3a(a^2r^4 + ar^2 + 12)}{4(ar^2 + 1)^3} \quad (13)$$

$$8\pi p_r = \frac{a\sqrt{4 + ar^2}\left(f_3(r) - f_1(r)\sqrt{4 + ar^2}\right)}{4(1 + ar^2)^2\left(f_2(r) - f_4(r)\right)} \quad (14)$$

$$\Delta = \frac{\sqrt{3}a^2r^2(ar^2 + 7)\left[f_4(r) - f_2(r)\right]^{-1}}{4(ar^2 + 1)^3\sqrt{ar^2 + 4}}$$
$$\times\left(f_6(r) - f_5(r)\sqrt{ar^2 + 4}\right) \quad (15)$$

$$8\pi p_t = 8\pi p_r + \Delta \quad (16)$$

where

$$f_1(r) = 3A\sqrt{ar^2(ar^2 + 4)} + \sqrt{3}Br(ar^2 + 16) \quad (17)$$

$$f_2(r) = A\sqrt{ar^2(ar^2+4)} + \sqrt{3}Br(ar^2+4) \qquad (18)$$

$$f_3(r) = 9\sqrt{2}\ Br(ar^2+4)\tanh^{-1}\left(\frac{\sqrt{ar^2+4}}{\sqrt{6}}\right) \qquad (19)$$

$$f_4(r) = 3Br\sqrt{2ar^2+8}\ \tanh^{-1}\left(\frac{\sqrt{ar^2+4}}{\sqrt{6}}\right) \qquad (20)$$

$$f_5(r) = \sqrt{3}A\sqrt{ar^2(ar^2+4)} + 2Br(ar^2+7) \qquad (21)$$

$$f_6(r) = 3\sqrt{6}Br(ar^2+4)\tanh^{-1}\left(\frac{\sqrt{ar^2+4}}{\sqrt{6}}\right) \qquad (22)$$

We can write the density and pressure gradients as

$$\frac{\mathrm{d}\rho}{\mathrm{d}r} = -\frac{3a^2r(a^2r^4+35)}{2(ar^2+1)^4} \qquad (23)$$

$$8\pi\frac{\mathrm{d}p_r}{\mathrm{d}r} = -\frac{ar\sqrt{ar^2}}{2g_7(x)\ (ar^2+1)^3}\left[3\sqrt{2}B\ \{(g_4(x)+g_5(x)\}\tanh^{-1}\left(\frac{\sqrt{ar^2+4}}{\sqrt{6}}\right)\right.$$

$$\left. -\sqrt{ar^2+4}\ \{g_1(x)+g_2(x)+g_3(x)\} - g_6(x)\right] \qquad (24)$$

$$8\pi\frac{\mathrm{d}p_t}{\mathrm{d}r} = -\frac{a^3r^5\sqrt{ar^2+4}}{4p_7(x)\ (ar^2+1)^4\ (ar^2(ar^2+4))^{3/2}}\left[-3\sqrt{2}B\ \{p_4(x)+p_5(x)\}\right.$$

$$\left. \tanh^{-1}\left(\frac{\sqrt{ar^2+4}}{\sqrt{6}}\right) + \sqrt{ar^2+4}\{p_1(x)+p_2(x)-p_3(x)\} + p_6(x)\right] \qquad (25)$$

Where $\qquad\qquad\qquad\qquad\qquad\qquad\qquad\qquad\qquad\qquad\qquad\qquad\qquad\qquad\qquad\qquad\qquad\qquad (26)$

$$g_1(x) = a^3r^4\left[3A^2\sqrt{\frac{ar^2(ar^2+4)}{(ar^2-2)^2}} + 3B^2r^2\sqrt{\frac{ar^2(ar^2+4)}{(ar^2-2)^2}} + 5\sqrt{3}ABr\right]$$

$$-708B^2\sqrt{\frac{ar^2(ar^2+4)}{(ar^2-2)^2}} \qquad (27)$$

$$g_2(x) = a^2r^2\left[15A^2\sqrt{\frac{ar^2(ar^2+4)}{(ar^2-2)^2}} + 81B^2r^2\sqrt{\frac{ar^2(ar^2+4)}{(ar^2-2)^2}} + 67\sqrt{3}ABr\right] \qquad (28)$$

$$g_3(x) = 2a\left[-21A^2\sqrt{\frac{ar^2(ar^2+4)}{(ar^2-2)^2}} + 90B^2r^2\sqrt{\frac{ar^2(ar^2+4)}{(ar^2-2)^2}} + 103\sqrt{3}ABr\right] \qquad (29)$$

$$g_4(x) = 24ar\left[3\sqrt{3}Br\sqrt{\frac{ar^2(ar^2+4)}{(ar^2-2)^2}} + 7A\right] - 412\sqrt{3}B\sqrt{\frac{ar^2(ar^2+4)}{(ar^2-2)^2}} \qquad (30)$$

$$g_5(x) = a^3r^5\left[5\sqrt{3}Br\sqrt{\frac{ar^2(ar^2+4)}{(ar^2-2)^2}} + 6A\right] + 3a^2r^3\left[19\sqrt{3}Br\sqrt{\frac{ar^2(ar^2+4)}{(ar^2-2)^2}} + 22A\right] \qquad (31)$$

$$g_6(x) = 54B^2\{a^2r^4+5ar^2-14\}\sqrt{\frac{ar^2(ar^2+4)^2}{(ar^2-2)^2}}\left[\tanh^{-1}\left(\frac{\sqrt{ar^2+4}}{\sqrt{6}}\right)\right]^2 \qquad (32)$$

$$g_7(x) = \left[A\sqrt{ar^2(ar^2+4)} + \sqrt{3}Br(ar^2+4) - 3Br\sqrt{2ar^2+8}\ \tanh^{-1}\left(\frac{\sqrt{ar^2+4}}{\sqrt{6}}\right)\right]^2 \qquad (33)$$

$$p_1(x) = 9a^3r^4\left[-4A^2\sqrt{\frac{ar^2(ar^2+4)}{(ar^2-2)^2}} + 22B^2r^2\sqrt{\frac{ar^2(ar^2+4)}{(ar^2-2)^2}} + 23\sqrt{3}ABr\right]$$

$$+a^5Br^9\left[6Br\sqrt{\frac{ar^2(ar^2+4)}{(ar^2-2)^2}}+\sqrt{3}A\right]+10368B^2\sqrt{\frac{ar^2(ar^2+4)}{(ar^2-2)^2}} \tag{34}$$

$$p_2(x)=2a^4r^6\left[12A^2\sqrt{\frac{ar^2(ar^2+4)}{(ar^2-2)^2}}+39B^2r^2\sqrt{\frac{ar^2(ar^2+4)}{(ar^2-2)^2}}+23\sqrt{3}ABr\right]$$

$$-4a\left[-168A^2\sqrt{\frac{ar^2(ar^2+4)}{(ar^2-2)^2}}+795B^2r^2\sqrt{\frac{ar^2(ar^2+4)}{(ar^2-2)^2}}+776\sqrt{3}ABr\right] \tag{35}$$

$$p_3(x)=2a^2r^2\left[180A^2\sqrt{\frac{ar^2(ar^2+4)}{(ar^2-2)^2}}+879B^2r^2\sqrt{\frac{ar^2(ar^2+4)}{(ar^2-2)^2}}+337\sqrt{3}ABr\right] \tag{36}$$

$$p_4(x)=\sqrt{3}a^5Br^{10}\sqrt{\frac{ar^2(ar^2+4)}{(ar^2-2)^2}}+4a^4r^7\left[11\sqrt{3}Br\sqrt{\frac{ar^2(ar^2+4)}{(ar^2-2)^2}}+12A\right]$$

$$+6208\sqrt{3}B\sqrt{\frac{ar^2(ar^2+4)}{(ar^2-2)^2}} \tag{37}$$

$$p_5(x)=a^3r^5\left[115\sqrt{3}Br\sqrt{\frac{ar^2(ar^2+4)}{(ar^2-2)^2}}+216A\right]-64a^2r^3\left[17\sqrt{3}Br\sqrt{\frac{ar^2(ar^2+4)}{(ar^2-2)^2}}+9A\right]$$

$$-4ar\left[439\sqrt{3}Br\sqrt{\frac{ar^2(ar^2+4)}{(ar^2-2)^2}}+672A\right] \tag{38}$$

$$p_6(x)=216B^2\left\{(2a^3r^6-3a^2r^4-30ar^2+56)\right\}\sqrt{\frac{ar^2(ar^2+4)^2}{(ar^2-2)^2}}\left[\tanh^{-1}\left(\frac{\sqrt{ar^2+4}}{\sqrt{6}}\right)\right]^2 \tag{39}$$

$$p_7(x)=\left[A\sqrt{\frac{ar^2(ar^2+4)}{(ar^2-2)^2}}(ar^2-2)+\sqrt{3}Br(ar^2+4)-3Br\sqrt{2ar^2+8}\right.$$

$$\left.\times\tanh^{-1}\left(\frac{\sqrt{ar^2+4}}{\sqrt{6}}\right)\right]^2. \tag{40}$$

These density and pressure gradients are represented graphically in Fig. 6.

Using the relationship between e^λ and mass $m(r)$ i.e.

$$e^{-\lambda}=1-\frac{2m}{r} \tag{41}$$

and (3) we get

$$m(r)=4\pi\int_0^r\rho r^2\mathrm{d}r=\frac{3ar^3(ar^2+4)}{8(ar^2+1)^2} \tag{42}$$

4   Conditions for physical viability of the solutions

The following conditions are to be fulfilled by the solution in order to represent a physically viable configuration.

1) The solution should be free from physical and geometric singularities, i.e. it should yield finite and positive values of the central pressure, central density and nonzero positive value of $e^\nu|_{r=0}$ and $e^\lambda|_{r=0}=1$.

2) The causality condition should be obeyed i.e. velocity of sound should be less than that of light throughout the model. In addition to the above the velocity of sound should be decreasing towards the surface i.e. $\dfrac{\mathrm{d}}{\mathrm{d}r}\dfrac{\mathrm{d}p_r}{\mathrm{d}\rho}<0$ or $\dfrac{\mathrm{d}^2p_r}{\mathrm{d}\rho^2}>0$ and $\dfrac{\mathrm{d}}{\mathrm{d}r}\dfrac{\mathrm{d}p_t}{\mathrm{d}\rho}<0$ or $\dfrac{\mathrm{d}^2p_t}{\mathrm{d}\rho^2}>0$ for $0\leqslant r\leqslant r_b$ i.e. the velocity of sound is increasing with the increase of density and it should be decreasing outwards.

3) The adiabatic index, $\gamma=\dfrac{\rho+p_r}{p_r}\dfrac{\mathrm{d}p_r}{\mathrm{d}\rho}$ for realistic matter should be $\gamma>4/3$.

4) The red-shift z should be positive, finite and mono-

tonically decreasing in nature with the increase of the radial coordinate.

5) For a stable anisotropic compact star, $0 < |v_t^2 - v_r^2| \leqslant 1$ must be satisfied, [40].

6) Anisotropy must be zero at the center and increas-ing outward.

5　Properties of the solution

The central values of p_r, p_t, ρ and the Zeldovich's condition can be written as

$$8\pi p_{rc} = 8\pi p_{tc} = \frac{a}{2}\left[-2\sqrt{a}\,A + 4\sqrt{3}\,B - 6\sqrt{2}\,B\tanh^{-1}(\sqrt{2/3})\right]$$
$$\times\left[36\sqrt{2}\,B\tanh^{-1}(\sqrt{2/3}) - 32\sqrt{3}\,B - 12\sqrt{a}\,A\right] > 0 \tag{43}$$

$$8\pi\rho_c = 9a > 0; \quad \forall\, a > 0 \tag{44}$$

$$\frac{p_{rc}}{\rho_c} = \frac{1}{18}\left[-2\sqrt{a}\,A + 4\sqrt{3}\,B - 6\sqrt{2}\,B\tanh^{-1}(\sqrt{2/3})\right]$$
$$\times\left[36\sqrt{2}\,B\tanh^{-1}(\sqrt{2/3}) - 32\sqrt{3}\,B - 12A\sqrt{a}\right] \leqslant 1. \tag{45}$$

Now using the two constraints on A, B and a given in (43) and (45), we get a final form as

$$\frac{8\sqrt{3} - 9\sqrt{2}\,\tanh^{-1}(\sqrt{2/3})}{3\sqrt{a}} < \frac{A}{B}$$
$$\leqslant \frac{13\sqrt{3} - 18\sqrt{2}\,\tanh^{-1}(\sqrt{2/3})}{6\sqrt{a}}. \tag{46}$$

Now the velocity of sound within the stellar object can be found as

$$v_r^2 = \frac{\mathrm{d}p_r/\mathrm{d}r}{\mathrm{d}\rho/\mathrm{d}r}, \quad v_t^2 = \frac{\mathrm{d}p_t/\mathrm{d}r}{\mathrm{d}\rho/\mathrm{d}r}. \tag{47}$$

The relativistic adiabatic index and the compression modulus is given by

$$\Gamma_r = \frac{\rho + p_r}{p_r}\,\frac{\mathrm{d}p_r}{\mathrm{d}\rho}; \quad \Gamma_t = \frac{\rho + p_t}{p_t}\,\frac{\mathrm{d}p_t}{\mathrm{d}\rho}. \tag{48}$$

For a static configuration at equilibrium Γ_r has to be more than $4/3$.

The generalized Tolman-Oppenheimer-Volkoff (TOV) equation was contributed by [41] as

$$-\frac{M_g(\rho + p_r)}{r^2}\,\mathrm{e}^{(\lambda - \nu)/2} - \frac{\mathrm{d}p_r}{\mathrm{d}r} + \frac{2(p_t - p_r)}{r} = 0 \tag{49}$$

provided

$$M_g(r) = \frac{1}{2}\,r^2\nu'\mathrm{e}^{(\nu - \lambda)/2}. \tag{50}$$

The above equation (49) can be written in terms of balanced force equation due to anisotropy (F_a), gravity (F_g) and hydrostatic (F_h) i.e.

$$F_g + F_h + F_a = 0. \tag{51}$$

Here

$$F_g = -\frac{M_g(\rho + p_r)}{r^2}\,\mathrm{e}^{(\lambda - \nu)/2} \tag{52}$$

$$F_h = -\frac{\mathrm{d}p_r}{\mathrm{d}r} \tag{53}$$

$$F_a = \frac{2(p_t - p_r)}{r}. \tag{54}$$

The generalized TOV equation (51) can be represent by a figure showing the forces that are balanced to each Fig. 13.

6　Boundary conditions

We assume that the exterior spacetime is the Schwarzschild solution, which has to match smoothly with the interior solution and is given by

$$\mathrm{d}s^2 = \left(1 - \frac{2M}{r}\right)\mathrm{d}t^2 - \left(1 - \frac{2M}{r}\right)^{-1}\mathrm{d}r^2$$
$$- r^2(\mathrm{d}\theta^2 + \sin^2\theta\,\mathrm{d}\phi^2). \tag{55}$$

By matching the interior solution (1) and exterior solution (55) at the boundary $r = r_b$ we get

$$\mathrm{e}^{\nu_b} = 1 - \frac{2M}{r_b}$$
$$= \left[A + \frac{B}{\sqrt{a}}\left\{\sqrt{12 + 3ar_b^2} - 3\sqrt{2}\right.\right.$$
$$\left.\left.\times\tanh^{-1}\left(\sqrt{\frac{4 + ar_b^2}{6}}\right)\right\}\right]^2 \tag{56}$$

$$\mathrm{e}^{-\lambda_b} = 1 - \frac{2M}{r_b} = \frac{\left(2 - ar_b^2\right)^2}{4\left(1 + ar_b^2\right)^2} \tag{57}$$
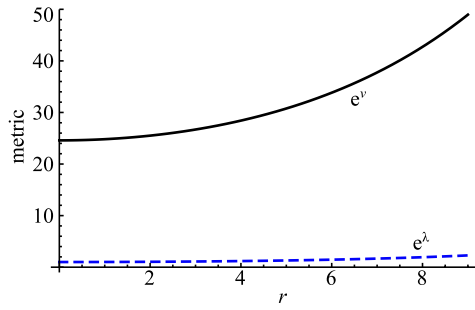
$$p_r(r_b) = 0. \tag{58}$$

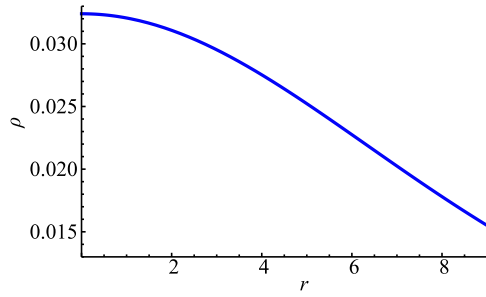Fig. 1.   Variation of metric potential with radius.

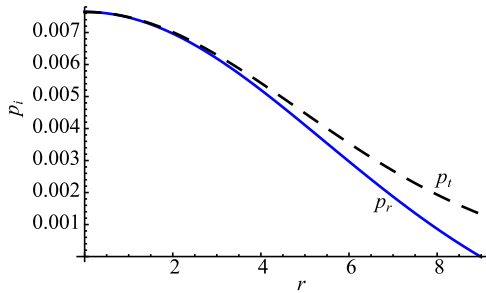Fig. 2.   Variation of density with radius.

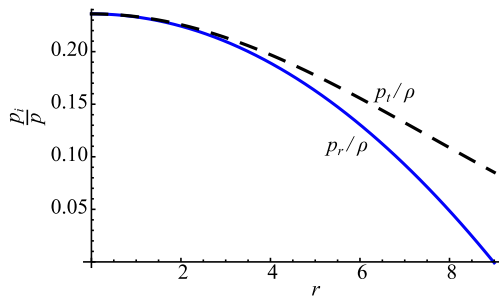Fig. 3.   Variation of pressures with radius.

Fig. 4.   Variation of pressure to density ratios with radius.
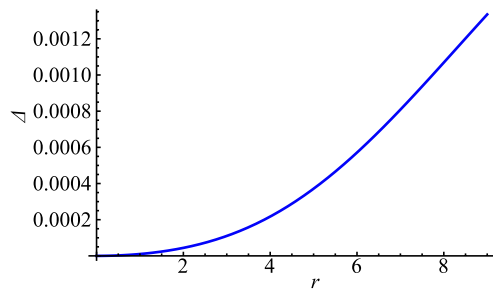
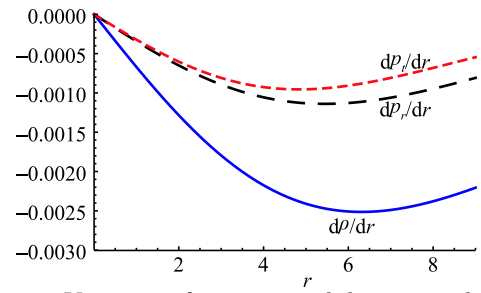Fig. 5.   Variation of anisotropy with radius.

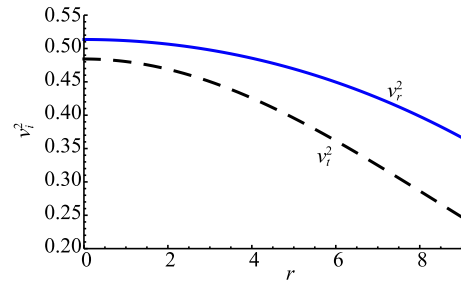Fig. 6.   Variation of pressure and density gradients with radius.

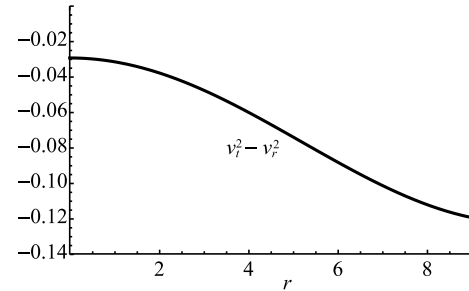Fig. 7.   Variation of square of sound speeds with radius.

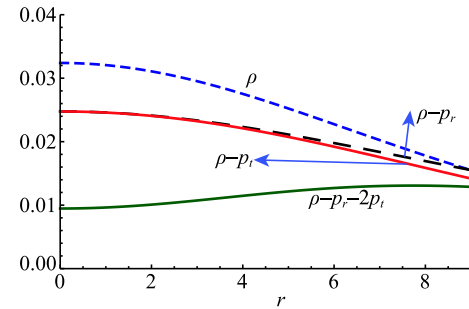Fig. 8.   Variation of stability factor with radius.

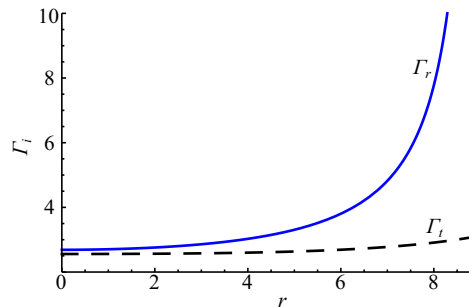Fig. 9.   Variation of energy conditions with radius.

Fig. 10.   Variation of adiabatic index with radius.

Table 1.   Optimization of masses, radii, Buchdahl limit, surface redshift and comparison with observed values.

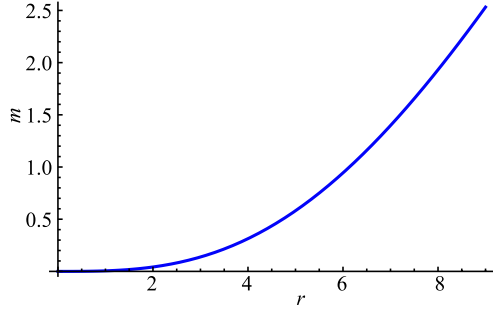| stars	a/km^{-2}	r_b/km	$M/M_\odot$	$2M/r_b$	z_s	$M_{obs}/M_\odot$	R_{obs}/km	type	Ref.
Cen X-3	0.00147	8.7	1.21	0.278	0.177	1.21 ± 0.21	–	NS	[42]
PSR J0348+0432	0.000751	13	2.01	0.309	0.203	2.01	13 ± 2	NS	[43]
PSR B0943+10	0.00077	2.6	0.02	0.0155	0.008	0.02	2.6	QS	[44]
XTE J1739-217	0.000934	10.9	1.51	0.277	0.176	1.51	10.9	QS	[45]

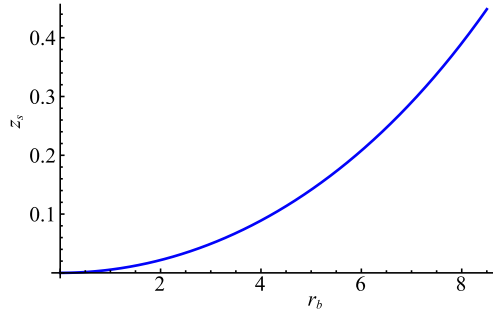Fig. 11.   Variation of mass with radius.

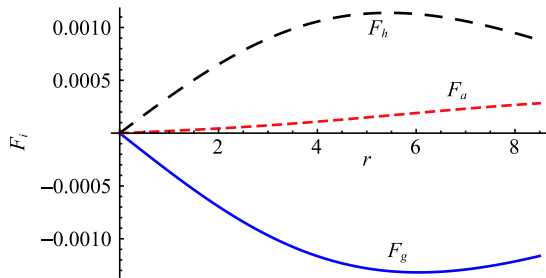Fig. 12.   Variation of surface redshift with radius.

Fig. 13.   Counter-balancing of three different forces acting in an anisotropic fluid sphere.

Using the boundary condition (56–58), we get

$$A = \frac{2-ar_b^2}{4(1+ar_b^2)} - \frac{B}{\sqrt{a}}\left[3\sqrt{2}\ \tanh^{-1}\left(\sqrt{\frac{4+ar_b^2}{6}}\right)\right.$$
$$\left. -\sqrt{12+3ar_b^2}\right], \tag{59}$$

$$\frac{2M}{r_b} = 1 - \frac{\left(2-ar_b^2\right)^2}{4\left(1+ar_b^2\right)^2}, \tag{60}$$

$$\frac{A}{B} = \left[3ar_b^2\sqrt{ar_b^2+4}\ \sqrt{\frac{ar_b^2(ar_b^2+4)}{(ar_b^2-2)^2}} - 6\sqrt{ar_b^2+4}\right.$$
$$\left.\sqrt{\frac{ar_b^2(ar_b^2+4)}{(ar_b^2-2)^2}}\ \right]^{-1}$$
$$\times \left[36\sqrt{2}\ r_b\ \tanh^{-1}\left(\sqrt{\frac{ar_b^2+4}{6}}\right) + 9\sqrt{2}\ ar_b^3\right.$$
$$\tanh^{-1}\left(\sqrt{\frac{ar_b^2+4}{6}}\right) - 16\sqrt{3}\ r_b\sqrt{ar_b^2+4}$$
$$\left. -\sqrt{3}ar_b^3\sqrt{ar_b^2+4}\right]. \tag{61}$$

Now the gravitational red-shift at the stellar surface is given by

$$z_s\ =\ \mathrm{e}^{-\nu_b/2} - 1 = \frac{2(1+ar_b^2)}{2-ar_b^2} - 1. \tag{62}$$

For a physically stable static configuration, the energy condition, such as Null Energy Condition (NEC), Weak Energy Condition (WEC), Strong Energy Condition (SEC) and Dominant Energy Condition, needs to be satisfied throughout the interior region i.e.

$$\rho \geqslant 0;\ \rho - p_r \geqslant 0;\ \rho - p_t \geqslant 0;$$
$$\rho - p_r - 2p_t \geqslant 0;\ \rho \geqslant (|p_r|,\ |p_t|). \tag{63}$$

7   Results and conclusions

It has been observed that the physical parameters $\left(p_r,\ p_t,\ \rho,\ p_r/c^2\rho,\ p_t/c^2\rho,\ v_r^2,\ v_t^2\right)$ are positive at the center and within the limit of a realistic equation of state and monotonically decreasing outward (Figs. 2−4, 7). However the metric potentials, anisotropy, surface redshift, mass-function and Γ are increasing outward, which is necessary for a physically viable configuration (Figs. 1, 5, 10–12).

Furthermore, our presented solution satisfies all the energy conditions which are needed by a physically possible configuration. The Strong Energy Condition (SEC), Weak Energy Condition (WEC), Null Energy Condition (NEC) and Dominant Energy Condition (DEC) are shown in Fig. 9. The stability factor $v_t^2 - v_r^2$

must lie in between -1 and 0 for a stable and between 0 and 1 for an unstable configuration. Therefore the presented solution satisfies the stability condition (Fig. 8).

The decreasing nature of pressures and density is further justified by their negativity of their gradients, Fig. 6. The solution represents a static and equilibrium configuration as the forces acting on the fluid sphere counterbalance each other. For an anisotropic stellar fluid in equilibrium the gravitational force, the hydro-static pressure and the anisotropic force are acting through the TOV-equation and counter-balancing each other, Fig. 13.

Using this solution, we have presented some models of well-known compact stars and compare their observed masses and radii with our calculated values, as shown in Table 1. Our presented models are in good agreement with the experimentally observed values, so the presented solution might have astrophysical significance in the future.

References

1 K. Schwarzschild, Math. Phys., **189**: (1916a)
2 K. Schwarzschild, Math. Phys., **424**: (1916b)
3 R. L. Bowers, E. P. T. Liang, Astrophys. J., **188**: 657–665 (1974)
4 J. D. Bekenstein, Phys. Rev. D, **4**: 2185–2190 (1971)
5 S. D. Maharaj, R. Maartens, Gen. Relativ. Gravit., **21**: 899–905 (1989)
6 R. Tikekar and K. Jotania, Int. J. Mod. Phys. D, **14**: 1037–1048 (2005)
7 M. Esculpi et al, Gen. Relativ. Gravit., **39**: 633–652 (2007)
8 P. C. Vaidya, Proc. Ind. Acad. Sci. A, **33**: 264–276 (1951)
9 N. O. Santos, Mon. Not. R. Astron. Soc., **216**: 403–410 (1985)
10 W. B. Bonnor, A. K. G. de Oliveira, and N. O. Santos, Phys. Rep., **181**: 269–326 (1989)
11 R. Sharma and R. Tikekar, Pramana J. of Phys., **79**: 501-509 (2012)
12 M. Govender et al, Astrophys. Space Sci., **361**: 33 (2016)
13 P. Bhar, Astrophys. Space Sci., **356**: 309–318 (2015)
14 P. Bhar, Eur. Phys. J. C, **75**: 123 (2015)
15 K. N. Singh and N. Pant, Astrophys. Space Sci., **358**: 44 (2015)
16 H. Andreasson, J. Phys.: Conference Series, **189**: 012001–0120013 (2009)
17 P. Takisa Mafa, S. Ray, S. D. Maharaj, Astrophys. Space Sci., **350**: 733 (2014)
18 S. A. Ngubelanga, S. D. Maharaj, and S. Ray, Astrophys. Space Sci., **357**: 74 (2015)
19 M. Govender and S. Thirukkanesh, Astrophys. Space Sci., **358**: 16–22 (2015)

20 P. Bhar and F. Rahaman, Euro. Phys. J. C, **75**: 41 (2015)
22 F.S.N. Lobo, Class. Quantum Grav., **23**: 1525 (2006)
23 F. Rahaman et al, Euro. Phys. J. C, **72**: 2071 (2012)
24 F. Rahaman et al, Gen. Relativ. Gravit., **44**: 107–124 (2012)
25 P. Bhar, Astrophys. Space Sci., **359**: 41 (2015)
26 P. H. Chavanis, T. Harko, Phys. Rev. D, **86**: 064011 (2012)
27 T. Harko, Phys. Rev. D, **68**: 064005 (2003)
28 N. Dadhich et al, Phys. Rev. D, **88**: 084024 (2013)
29 P. S. Joshi and D. Malafarina, Int. J. Mod. Phys. D, **20**: 2641–2729 (2011)
30 N. Dadhich et al, Phys.Lett. B, **711**: 196–198 (2012)
31 S. Hansraj et al, Eur. Phys. J. C, **75**: 277 (2015)
32 S. D. Maharaj et al, Phys. Rev. D, **91**: 084049 (2015)
33 N. Dadhich et al, Phys. Rev. D, **93**: 044072 (2016)
34 A. Banerjee et al, Euro. Phys. J. C, **76**: 34 (2016)
35 K. R. Karmarkar, Proc. Indian. Acad. Sci. A, **27**: 56-60 (1948)
36 K. N. Singh and N. Pant, Astrophys. Space Sci., **361**: 177 (2016)
37 K. N. Singh et al, Astrophys. Space Sci., **361**: 173 (2016)
38 S. Thakadiyil and M. K. Jasim, Int. J. Theor. Phys., **52**: 3960–3964 (2013)
39 S.N. Pandey and S. P. Sharma, Gene. Relativ. Gravit., **14**: 113–115 (1981)
40 L. Herrera and N. O. Santos, Phys. Rep., **286**: 53–130 (1997)
41 J. Ponce de Leon, Gen. Relativ. Gravit., **19**: 797–807 (1987)
42 T. D. C. Ash et al, Gen. Relativ. Gravit., **307**: 357–364 (1999)
43 J. Antoniadis et al, Science, **340**: 1233232 (2013)
44 Y. L. Yue et al, Astrophys. J., **649**: L95–L98 (2006)
45 C. M. Zhang et al, Publ. Astron. Soc. Pac., **119**: 1108–1113 (2007)